Pyruvate Ferredoxin Oxidoreductases of the Hyperthermophilic Archaeon, *Pyrococcus furiosus*, and the Hyperthermophilic Bacterium, *Thermotoga maritima*, Have Different Catalytic Mechanisms†

Eugene T. Smith, Jenny M. Blamey, and Michael W. W. Adams*

Department of Biochemistry and Center for Metalloenzyme Studies, University of Georgia, Athens, Georgia 30602

Received August 4, 1993; Revised Manuscript Received November 17, 1993®

ABSTRACT: Pyruvate ferredoxin oxidoreductase (POR) has been previously purified from two hyperthermophiles, the archaeon *Pyrococcus furiosus* (Pf, T_{opt} = 100 °C) and the bacterium *Thermotoga maritima* (Tm, T_{opt} = 80 °C). Each catalyzes the oxidative decarboxylation of pyruvate to acetyl-CoA and CO_2 near the optimal growth temperature of the organism and are virtually inactive at 25 °C. Both PORs contain a thiamine pyrophosphate (TPP) cofactor and at least two [4Fe–4S] ferredoxin-type clusters. We have now shown, using EPR spectroscopy and metal analyses, that Pf POR also contains an unusual copper center that is not present in Tm POR. In addition, distinct catalytic intermediates were generated in both enzymes by the addition, separately and in combination, of the substrates pyruvate and CoASH, and these were examined by EPR spectroscopy. The addition of pyruvate to oxidized Pf POR produced an isotropic signal centered at g = 2.01, which was measurably broader in the presence of pyruvate-2-^{13}C. This signal, which was assigned to a (hydroxyethyl)thiamine pyrophosphate radical intermediate, was not observed in Tm POR under the same experimental conditions. Incubation of the oxidized enzymes with CoASH resulted in the partial reduction of the copper site in Pf POR and the partial reduction of a novel iron–sulfur center in Tm POR, which was not seen in the dithionite-reduced enzyme. The addition of both pyruvate and CoASH to the PORs in their oxidized states resulted in the reduction of the same iron–sulfur centers that are reduced by sodium dithionite. On the basis of these observations, two distinct catalytic mechanisms are proposed for pyruvate oxidation by these two hyperthermophilic enzymes.

Microorganisms have recently been isolated near marine hydrothermal vents that have the remarkable property of optimal growth near and even above 100 °C (Stetter *et al.*, 1990; Adams & Kelly, 1992; Adams, 1993). Most of the biochemical studies with these so-called hyperthermophiles have focused on the archaeon (formerly archaebacterium), *Pyrococcus furiosus* (Pf[1]; Fiala & Stetter, 1986), and the (eu)bacterium, *Thermotoga maritima* (Tm; Huber *et al.*, 1986), which grow at up to 105 and 90 °C, respectively. Several of the enzymes involved in sugar fermentation have been purified from the two hyperthermophiles (Adams, 1992, 1993). These include hydrogenase (Bryant & Adams, 1989), ferredoxin (Aono *et al.*, 1989), aldehyde ferredoxin oxidoreductase (Mukund & Adams, 1991), and pyruvate ferredoxin oxidoreductase (POR; Blamey & Adams, 1993) from *P. furiosus* and hydrogenase (Jusczcak *et al.*, 1992), lactate dehydrogenase (Wrba *et al.*, 1990a), glyceraldehyde-3-phosphate dehydrogenase (Wrba *et al.*, 1990b), and pyruvate ferredoxin oxidoreductase (Blamey & Adams, 1994) from *T. maritima*. All of these enzymes are thermostable and require elevated temperatures (>90 °C) for optimal catalytic activity. It is not known how they catalyze reactions at temperatures where most other proteins, cofactors, and substrates are unstable. In addition, there is evidence that the hyperthermophiles are the earliest known ancestors of all extant life on this planet (Woese *et al.*, 1990), having evolved when the earth was much hotter than it is today. Therefore, an understanding of the catalytic mechanisms of hyperthermophilic enzymes is important from both a biochemical and an evolutionary point of view.

The final oxidative step in carbohydrate fermentation by hyperthermophiles such as *P. furiosus* and *T. maritima* is catalyzed by pyruvate ferredoxin oxidoreductase. This involves the oxidative decarboxylation of pyruvate according to the following half-reaction:

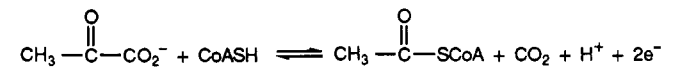

This is coupled to the two-electron reduction of POR, which in turn reduces the redox protein ferredoxin. Pf POR and Tm POR are heterotetramers with M_r values of approximately 115 000. Each contains at least two [4Fe–4S] ferredoxin-type clusters and thiamine pyrophosphate (TPP) as a cofactor (Blamey & Adams, 1993, 1994). In contrast, the PORs that have been purified from mesophilic anaerobes are homodimers of M_r 240 000, although they also contain TPP and multiple [4Fe–4S] clusters [see Blamey and Adams (1994)].

Pyruvate-oxidizing enzymes can be classified generally as either PORs, which are typically found in anaerobic microorganisms [see Blamey and Adams (1994)], or as pyruvate dehydrogenase complexes, which are only found in aerobic organisms [e.g., Guest *et al.* (1991)]. Although POR and the pyruvate dehydrogenase complex are fundamentally different in structure, the mechanism of the latter enzyme complex is well understood and may provide insight into the poorly

† This research was supported by a grant from the U.S. Department of Energy (FG09-88ER13901) and by a National Science Foundation Training Group Award to the Center for Metalloenzyme Studies of the University of Georgia (DIR 9014281).

* Author to whom correspondence should be addressed. Telephone: (706) 542-2060. FAX: (706) 542-0229. E-MAIL: ADAMSM@-BSCR.CC.UGA.EDU.

® Abstract published in *Advance ACS Abstracts,* January 1, 1994.

[1] Abbreviations: TPP, thiamine pyrophosphate; HETPP, (hydroxyethyl)thiamine pyrophosphate; Pf, *Pyrococcus furiosus*; Tm, *Thermotoga maritima*; POR, pyruvate ferredoxin oxidoreductase; CoASH, coenzyme A; ICP-AES, inductively coupled plasma atomic emission spectroscopy.

0006-2960/94/0433-1008$04.50/0

Scheme 1: Proposed Pathway for Pyruvate Oxidation by Pyruvate Dehydrogenase Complex Illustrating the Formation of (I) TPP Anion, (II) HETPP Anion, (III) Acetyllipoic Acid, and (IV) Acetyl-CoA

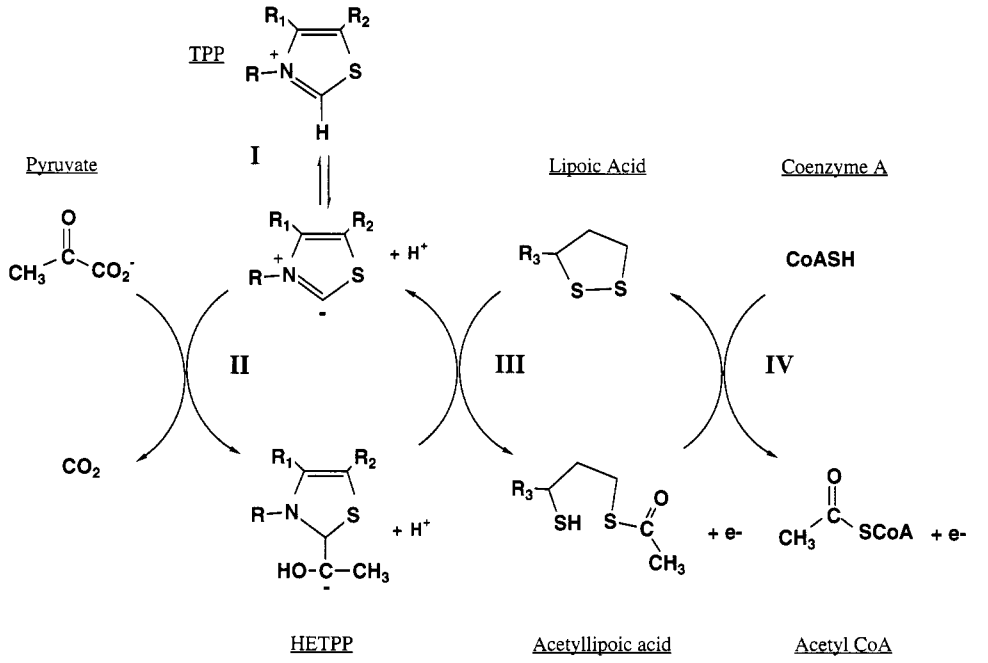

understood catalytic mechanism of POR. Key steps in the oxidative catalysis of pyruvate by the three distinct enzymes of the pyruvate dehydrogenase complex are summarized in Scheme 1. Briefly, pyruvate dehydrogenase contains TPP and catalyzes the formation of a (hydroxyethyl)thiamine pyrophosphate (HETPP) intermediate (Scheme 1, steps I and II); dihydrolipoamide acetyltransferase contains lipoic acid and catalyzes the formation of acetyl-CoA (steps III and IV); and dihydrolipoamide dehydrogenase contains FAD and serves as a final two-electron acceptor (steps III and IV).

At present it is not known whether the conventional TPP intermediates found in the pyruvate dehydrogenase complex participate in catalysis by POR. For example, in the 2-oxo acid:ferredoxin oxidoreductase from *Halobacterium halobium*, a novel (hydroxyalkyl)thiamine diphosphate radical was proposed as an intermediate (Kerscher & Oesterhelt, 1981). In addition, it is not known how POR catalyzes the formation of acetyl-CoA. A major problem is that a moiety equivalent to lipoic acid, which catalyzes the formation of acetyl-CoA from a TPP intermediate in the pyruvate dehydrogenase complex (Scheme 1, step III), has not been identified in any POR. On the other hand, it is assumed that the [4Fe–4S] centers found in PORs each serve as a single-electron acceptor and that they serve the same function as FAD, which is the final electron acceptor in the pyruvate dehydrogenase complex (Scheme 1, steps III and IV). In order to address the fundamental question of pyruvate oxidation by POR and how this differs from that of the pyruvate dehydrogenase complex, we have utilized the hyperthermophilic PORs recently purified from *P. furiosus* (Blamey & Adams, 1993) and *T. maritima* (Blamey & Adams, 1994). Specifically, catalytic intermediates were generated by the addition, separately and in combination, of pyruvate and CoASH to each POR, and these intermediates were examined by EPR spectroscopy. Surprisingly, the results indicate a catalytic role for copper in Pf POR and indicate that these two hyperthermophilic PORs oxidize pyruvate by two very different mechanisms. Pf POR appears to have a Cu/TPP radical-based mechanism for pyruvate oxidation, while Tm POR utilizes an FeS/TPP-based chemistry to catalyze the same reaction.

MATERIALS AND METHODS

Pyrococcus furiosus (DSM 3638) and *Thermotoga maritima* (DSM 3109) were both grown in a 400-L fermentor (Bryant & Adams, 1989; Jusczcak *et al.*, 1991). *P. furiosus* ferredoxin was purified as previously described (Aono *et al.*, 1989). Both PORs were purified under strict anaerobic conditions using buffers containing sodium dithionite (2 mM) and dithiothreitol (2 mM), as previously described (Blamey & Adams, 1993, 1994). Enzyme activities were determined by the pyruvate- and CoASH-dependent reduction of methyl viologen at 80 °C (Blamey & Adams, 1993). Multiple elemental analysis was performed by inductively coupled plasma atomic emission spectroscopy (ICP-AES) using a Jarrel Ash Plasma Comp 750 plasma emission spectrometer within the Department of Ecology of the University of Georgia. Serial dilutions of concentrated protein solutions (>50 mg/mL) were analyzed together with a serial dilution of a standard solution consisting of 10 mg/mL bovine serum albumin supplemented with W, Cu, Ni, or Fe, each at a final concentration of 100 ppm.

All manipulations of the pure PORs were performed under strict anaerobic conditions. Sodium dithionite and dithiothreitol were removed from the proteins by washing with at least 20 vol of 50 mM Tris-HCl (pH 8.0) and ultrafiltration using a PM-30 membrane (Amicon Co., Lexington, MA). Each POR was then oxidized under anaerobic conditions by adding either dichloroindophenol or thionine until the solution remained blue. The dye was subsequently removed by ultrafiltration and washing with the same anaerobic buffer until the eluant contained no visible traces of dye. No significant loss of activity was observed using this oxidation procedure. To prepare samples for EPR spectroscopy, stock solutions of Pf POR (310 μM) and Tm POR (225 μM) were first divided into 250-μL aliquots. A concentrated solution of substrate, e.g., CoASH, sodium pyruvate, or sodium pyruvate-2-^{13}C (Isotec, Inc., Miamisburg, OH), was then added to a final concentration of 20 mM under anaerobic conditions at 23 °C. These solutions were incubated at 80 °C for 2 min, injected into anaerobic stoppered quartz EPR tubes,

and frozen by plunging the tubes into heptane maintained at −60 °C by the addition of liquid nitrogen.

EPR spectra were recorded on an IBM-Bruker ER 300E spectrometer interfaced to an ESP 3220 data system and equipped with an Oxford Instruments ITC-4 flow cryostat. Spin quantitations were determined by double integration of the first derivative spectra recorded at 8 K using 10 μW of microwave power (Aasa & Vänngård, 1975). These were compared with the spectra of Cu (1 mM) in EDTA (100 mM) recorded under identical conditions.

RESULTS

Metal Analysis of PORs. It was previously reported that Pf POR and Tm POR contained approximately 8 and 10 Fe atoms/molecule, respectively (Blamey & Adams, 1993,1994). In this study, preliminary EPR analysis indicated the presence of copper in Pf POR (see below); therefore, both enzymes were examined by ICP-AES. It was found that Pf POR contained approximately 8 Fe, 1 Cu, and 2 Zn atoms/molecule. Boron and silicon were also found in significantly high concentrations in Pf POR. In fact, the ratio of iron, copper, zinc, boron, and silicon (8:1:2:6:4) remained constant despite serial dilutions, and none of these elements were detected at significant concentrations in the buffers. Pf POR treated with 5 mM EDTA and passed through a gel filtration column still contained stoichiometric amounts of copper. In addition, the same amounts of copper were detected in Pf POR samples from eight different purification procedures. However, copper, zinc, boron, and silicon were not detected in Tm POR by the same techniques employed to analyze Pf POR. The significance of boron and silicon in the latter enzyme is not known. The nature and proposed role of copper in Pf POR are described below.

EPR Spectroscopy. Both Pf POR and Tm POR in their oxidized states were treated with pyruvate, CoASH, or both at 80 °C for 2 min and then rapidly frozen for analysis by EPR spectroscopy. The spectra obtained are shown in Figures 1–4. For comparison purposes, these spectra were recorded under identical conditions and normalized to the same gain at various temperatures. Changes observed in the spectra of the oxidized enzymes as a function of temperature, microwave power, or the presence of one or both substrates are described below.

Oxidized POR. EPR spectra of the oxidized forms of Pf POR and Tm POR are shown in Figure 1. Oxidized Pf POR gave rise to a minor, fast-relaxing isotropic signal centered at $g = 2.016$, which was seen up to 20 K, and superimposed upon this was a broad signal centered at $g = 2.073$, which was observed above 30 K (Figure 1a). In addition, all samples exhibited a low-intensity feature at $g = 4.3$ (data not shown), which was attributed to Fe(III), and a very weak resonance near $g = 1.96$ (see Figure 1a), the source of which is not known. Due to both the low spin concentration (<0.1 spin/mol) and the relaxation properties of the feature at $g = 2.016$, it was previously assigned to an oxidized 3Fe cluster thought to be generated from the partial oxidative degradation of a [4Fe–4S] center (Blamey & Adams, 1993). However, the major feature of the spectrum of oxidized Pf POR centered at $g = 2.073$ (Figure 1a) was assigned to a Cu^{2+} center: its characteristic hyperfine resonances can be seen clearly in Figure 5. The g values of the hyperfine resonances (2.499, 2.368, and 2.251), the large parallel hyperfine splitting $A_{\parallel} = 150$ G, and the lack of visible absorption at 600 nm are all characteristic of a type 2 copper center of the type found, for example, in superoxide dismutase. In contrast, blue copper proteins have greatly reduced hyperfine splitting, strong visible absorption at 600 nm, and characteristically high reduction potentials (Solomon & Lowery, 1993). Spin quantitation showed that the signal from the copper site in Pf POR accounted for approximately 0.2 spin/mol. In contrast, the oxidized form of Tm POR gave rise to a fast-relaxing isotropic signal centered at $g = 2.017$, and this represented 0.06 spin/mol. This signal was also attributed to trace amounts of an oxidized [3Fe–4S] cluster, arising from the partial oxidative degradation of a [4Fe–4S] center (Blamey & Adams, 1994).

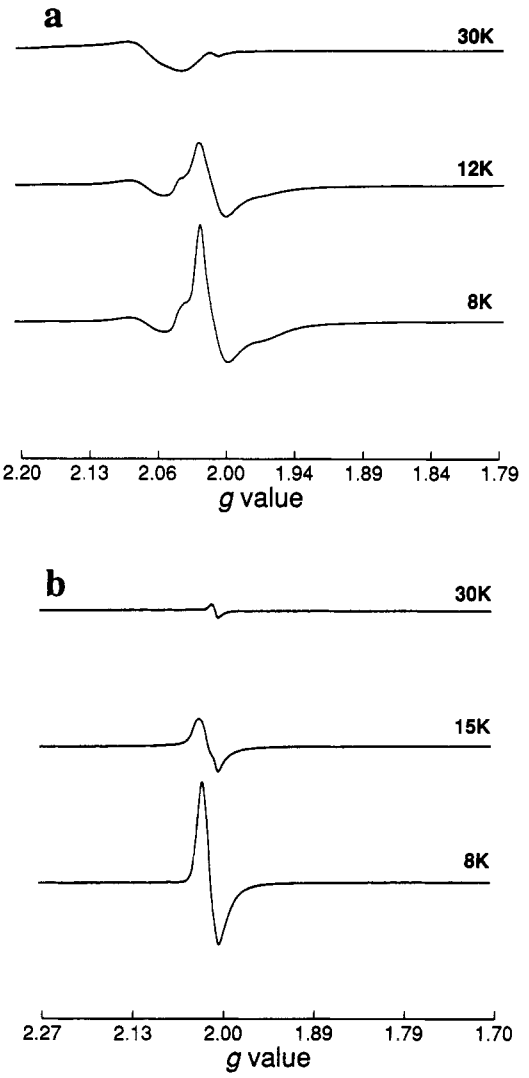

FIGURE 1: EPR spectra of oxidized (a) Pf POR at 8, 12, and 30 K and (b) Tm POR recorded at 8, 15, and 30 K in 50 mM Tris-HCl (pH 8). Experimental conditions were as follows: microwave power, 20 mW; modulation amplitude, 5 G; microwave frequency, 9.44 GHz; normalized to a gain of (a) 5×10^4 and (b) 2.5×10^4.

Effect of Pyruvate. As shown in Figure 2a, the addition of pyruvate to oxidized Pf POR induced an isotropic signal centered at $g = 2.012$ that was readily seen at 30 K, as well as an increase in the signal intensity at $g = 2.069$ from the Cu^{2+} center (compare with Figure 1a). Spin quantitation of the spectrum recorded at 10 μW and 8 K yielded a value of 0.70 spin/mol. As shown in Figure 6, the sharp isotropic signal ($g = 2.012$) was measurably broadened in the presence of pyruvate-2-^{13}C, indicating that this radical-type EPR signal is associated with the product of pyruvate decarboxylation, which can be reasonably assigned to an HETPP radical intermediate. In contrast, pyruvate added to the oxidized form of Tm POR caused only a slight change in the isotropic signal centered at $g = 2.017$ (Figure 2b), and this still accounted

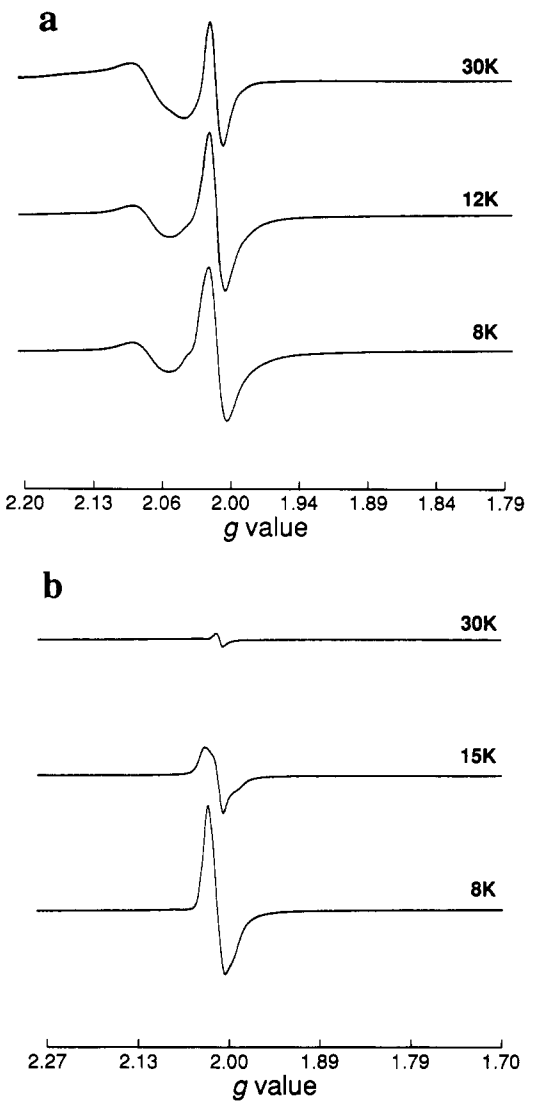

FIGURE 2: EPR spectra resulting from the addition of sodium pyruvate (final concentration, 20 mM) to (a) oxidized Pf POR recorded at 8, 12, and 30 K and (b) oxidized Tm POR recorded at 8, 15, and 30 K in 50 mM Tris-HCl. Experimental conditions were as follows: microwave power, 20 mW; modulation amplitude, 5 G; microwave frequency, 9.44 GHz; normalized to a gain of (a) 5×10^4 and (b) 2.5×10^4.

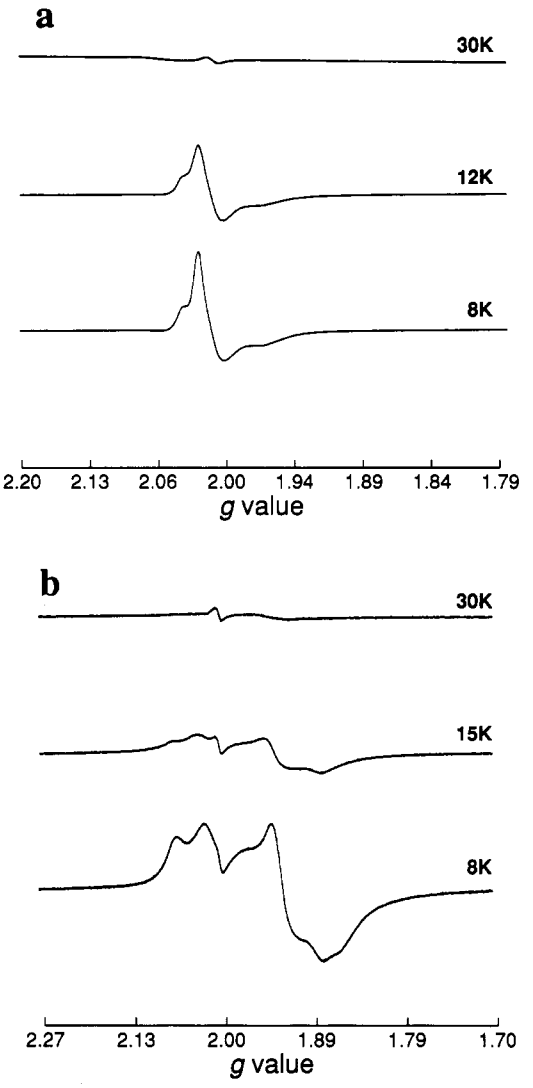

FIGURE 3: EPR spectra resulting from the addition of CoASH (final concentration, 20 mM) to (a) oxidized Pf POR recorded at 8, 12, and 30 K and (b) oxidized Tm POR recorded at 8, 15, and 30 K in 50 mM Tris-HCl (pH 8). Experimental conditions were as follows: microwave power, 20 mW; modulation amplitude, 5 G; microwave frequency, 9.44 GHz; normalized to a gain of (a) 5×10^4 and (b) 2.5×10^4.

for less than 0.06 spin/mol. The trace amount of oxidized 3Fe cluster present in the oxidized enzyme was therefore essentially unaffected by pyruvate. Accordingly, the spectra of oxidized Tm POR treated with pyruvate or pyruvate-*2*-^{13}C were identical.

Effect of CoASH. When oxidized Pf POR was incubated with CoASH, the rapidly relaxing isotropic signal ($g = 2.016$) assigned to an oxidized 3Fe center persisted, but the signal at $g = 2.073$ arising from the Cu^{2+} species disappeared (Figure 3a). The spectrum accounted for 0.07 spin/mol. Thus, the trace amount of oxidized 3Fe cluster was unaffected by pyruvate addition, but this caused the reduction of the copper site. In contrast, the addition of CoASH to oxidized Tm POR induced a fast-relaxing rhombic-type EPR signal characteristic of at least one reduced [4Fe–4S] center (Figure 3b). Spin quantitation showed that this signal represented 0.3 spin/mol. Although the EPR signal from the small amount of oxidized 3Fe center was still visible (compare Figures 1b and 3b), the CoASH-induced signal appeared to consist of a rhombic-type spectrum ($g_z = 2.028$, $g_y = 1.940$, and $g_x = 1.895$, now termed the $g = 2.03$ spectrum) that had been seen previously from dithionite-reduced Tm POR (Blamey & Adams, 1993; see Figure 7), but the predominant feature was a new rhombic spectrum with $g_z = 2.070$, $g_y = 1.930$, and $g_x = 1.864$ (the $g = 2.07$ signal).

Thus, the addition of CoASH appears to result in the reduction of at least one [4Fe–4S] center in Tm POR, but the [4Fe–4S] centers in Pf POR were unaffected (Figure 3). To further investigate whether CoASH would bind to and/or reduce other [4Fe–4S] centers, we used Pf ferredoxin in a control experiment. This small protein ($M_r = 7500$) contains a single 4Fe center which, because of incomplete cysteinyl ligation [see Conover *et al.* (1990)], is able to bind exogenous ligands such as cyanide (Conover *et al.*, 1991). However, no changes were observed when a 50-fold molar excess of CoASH was added to either oxidized or dithionite-reduced Pf ferredoxin (300 μM). Similarly, the spectrum of oxidized Tm POR was unaffected by the addition of a 50-fold molar excess of cyanide. These data suggest that the putative CoASH-binding 4Fe center of Tm POR, which in the reduced form exhibits the $g = 2.07$ rhombic signal, is apparently unique and structurally dissimilar to the cyanide-binding 4Fe center of Pf ferredoxin.

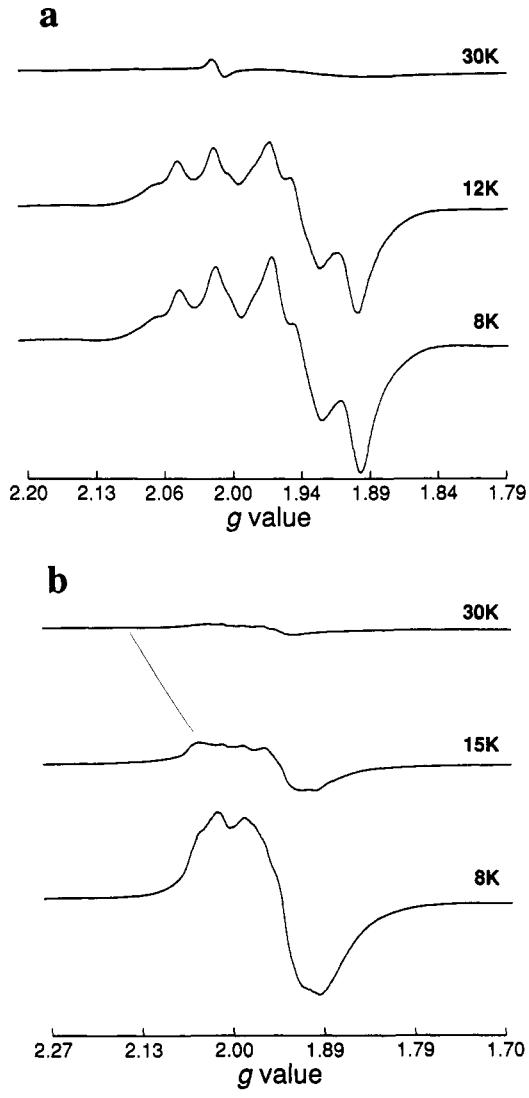

FIGURE 4: EPR spectra resulting from the addition of CoASH and sodium pyruvate (each at 20 mM final concentration) to (a) oxidized Pf POR recorded at 8, 12, and 30 K in 50 mM Tris-HCl (pH 8) and (b) oxidized Tm POR recorded at 8, 15, and 30 K. Experimental conditions were as follows: microwave power, 20 mW; modulation amplitude, 5 G; microwave frequency, 9.44 GHz; normalized to a gain of (a) 5×10^4 and (b) 8×10^3.

Effect of Pyruvate and CoASH. In principle, the addition of both substrates to oxidized POR in the absence of an external electron acceptor should result in a single turnover and the two-electron reduction of the enzyme. Hence, as shown in Figure 4, the addition of both CoASH and pyruvate to the oxidized forms of Pf POR and Tm POR induced spectral features characteristic of more than one reduced [4Fe–4S] center in each case. Spin quantitation of substrate-reduced Pf and Tm PORs yielded values of 0.82 and 1.30 spins/mol, respectively. With Pf POR, no differences were observed between the spectra of the enzyme reduced with either dithionite (Blamey & Adams, 1993) or pyruvate plus CoASH (Figure 4a). These spectra arise from the superposition of two rhombic EPR signals (A and B) from two distinct [4Fe–4S] centers, with $g_{z,y,x}$ values of 2.072, 1.941, and 1.895 for signal A and 2.053, 1.934, and 1.895 for signal B (note that previously, the g_x for signal B had been tentatively assigned a value of 1.79; Blamey & Adams, 1993).

In contrast, there were differences in the EPR spectra of Tm POR when it was reduced either by dithionite or by the two substrates (Figure 7), although in each case the spectrum represented approximately 1.3 spins/mol. From Figures 4 and 7 [see also Figure 5 of Blamey and Adams (1994)], both spectra appear to arise from the superposition of two rhombic-type signals, with respective $g_{z,y,x}$ values of 2.047, 1.930, and 1.890 (now termed the $g = 2.05$ signal) and 2.028, 1.940, and 1.890 (the $g = 2.03$ signal). In the spectrum of the dithionite-reduced enzyme, the $g = 2.05$ signal was slightly more intense than it was in the spectrum of the enzyme reduced by substrates (Figure 7). However, addition of CoASH to the dithionite-reduced enzyme generated a spectrum that was indistinguishable from that of the pyruvate/CoASH-reduced enzyme. On the other hand, the $g = 2.07$ rhombic spectrum (Figure 3b) exhibited by CoASH-treated Tm POR was not seen from the enzyme treated with both CoASH and pyruvate or both CoASH and dithionite (Figure 4b). In particular, the spectra of the latter two samples lacked the characteristic upward absorption feature at $g = 1.947$ seen in the CoASH-reduced enzyme, as well as the $g_z = 2.070$ resonance. Thus, reduced Tm POR appears to exhibit three distinct rhombic EPR signals: the $g = 2.05$ and 2.03 signals are both seen from the dithionite- and CoASH/pyruvate-reduced enzyme, while the CoASH-reduced form uniquely gives rise to the $g = 2.07$ signal. These signals presumably arise from three distinct FeS centers rather than from the spin-coupling of two such centers, although EPR studies at different frequencies will be required to confirm this. As with the oxidized Tm enzyme, no spectral changes were observed after the addition of a 50-fold excess of cyanide to dithionite-reduced Tm POR; hence the 4Fe-type center reduced by CoASH does not appear to bind cyanide as an exogenous ligand.

DISCUSSION

The surprising conclusions from the results presented here are that copper is an integral part of Pf POR and appears to participate directly in catalyzing acetyl-CoA production, yet this element is not present in Tm POR. Zinc, boron, and silicon were also found in stoichiometric amounts in Pf POR, but not in Tm POR. Since boron and silicon are major constituents of glass, it cannot be ruled out that these elements are contaminants, although why they should be found in one enzyme and not the other is puzzling.

There are, however, several lines of evidence supporting copper as a fundamental component of Pf POR. These include the following: (a) it is found in stoichiometric amounts, as determined by ICP-AES; (b) it could not be removed from the protein by gel filtration using EDTA-containing buffer; (c) copper has not been found in several other redox enzymes that have been purified from *P. furiosus* [see Adams (1992, 1993)]; and (d) the Cu^{2+} site in Pf POR was partially oxidized by pyruvate (Figures 2 and 5) and was reduced by CoASH (Figure 3). Furthermore, the purification of Pf POR involves at least four chromatography steps where the columns are equilibrated with Tris-HCl buffer, a known chelator of copper (McPhail & Goodman, 1984). Although seldom found in low-potential systems, copper has been detected in both the nickel–iron–sulfur-containing hydrogenase of *Methanobacterium formicicum* (Adams *et al.*, 1986) and the iron–sulfur NADH oxidase of *Acholeplasma laidawii* (Reinards *et al.*, 1981). Interestingly, in the latter case, copper was determined to be an EPR-silent cofactor (Reinards *et al.*, 1981).

In addition to ferredoxin-type [4Fe–4S] centers, both Pf and Tm PORs contained trace amounts of an oxidized 3Fe center. However, this will not be discussed in mechanistic terms, as its spin concentration (much less than 0.1 spin/mol) was so much lower than the other paramagnetic centers and

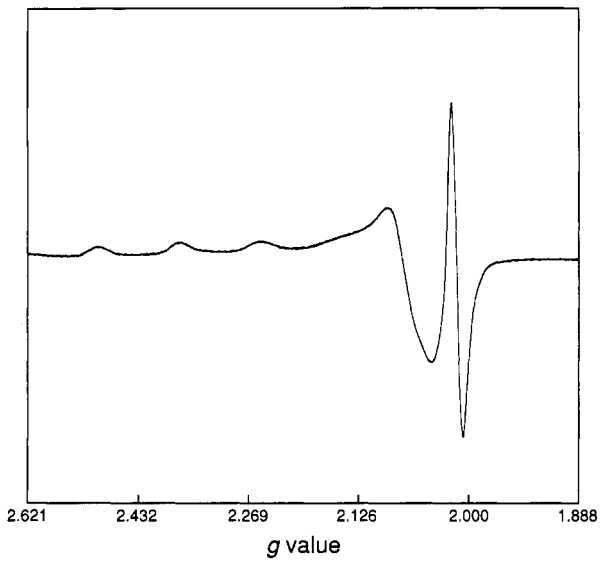

FIGURE 5: EPR spectrum resulting from the addition of sodium pyruvate (final concentration, 20 mM) to oxidized Pf POR recorded at 30 K in 50 mM Tris-HCl (pH 8). Experimental conditions were as follows: microwave power, 20 mW; modulation amplitude, 5 G; microwave frequency, 9.44 GHz; gain of 2.5×10^4.

Scheme 2: Proposed Pathway for Pyruvate Oxidation by *P. furiosus* POR Illustrating a Hypothetical Cu^{2+}/TPP Radical (I) and the Formation of (II) a HETPP Radical Intermediate, (III) Cu–SCoA complex, and (IV) Acetyl-CoA

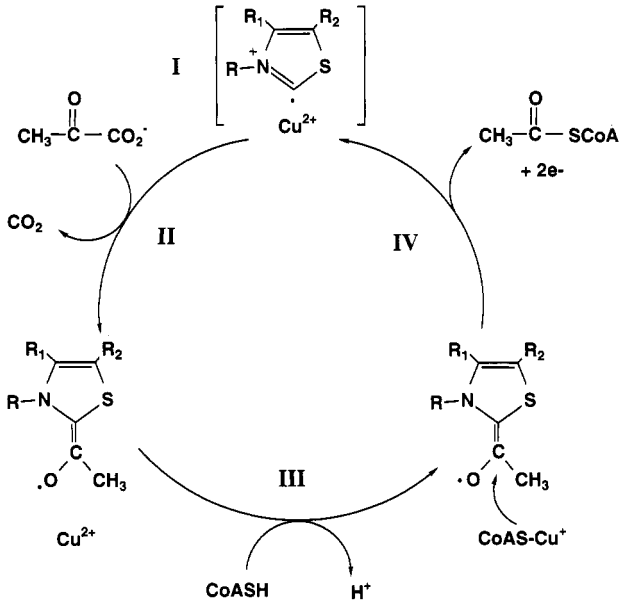

it was unaffected by the addition of CoASH or pyruvate. The less than integer spin concentrations observed for the other EPR-active species are attributed (unless stated otherwise) to either the loss of the loosely associated TPP cofactor, incomplete reduction, the unavoidable partial oxidative degradation of iron–sulfur centers, or a combination of these effects.

In the following, two distinct mechanisms are formulated for pyruvate oxidation: one by Pf POR (Scheme 2) and the other by Tm POR (Scheme 3). These are discussed in terms of the substrate-induced intermediates observed by EPR spectroscopy. Clearly, the spectroscopic data cannot be accounted for by the mechanism of pyruvate dehydrogenase shown in Scheme 1. In fact, it appears that the lipoic acid in this enzyme (Scheme 1) is replaced by metal centers in the PORs, namely, by copper in Pf POR (Scheme 2) and by an

Scheme 3: Proposed Pathway for Pyruvate Oxidation by *T. maritima* POR Illustrating the Formation of (I) TPP Anion, (II) HETPP Intermediate, (III) FeS–CoASH Complex, and (IV) Acetyl-CoA

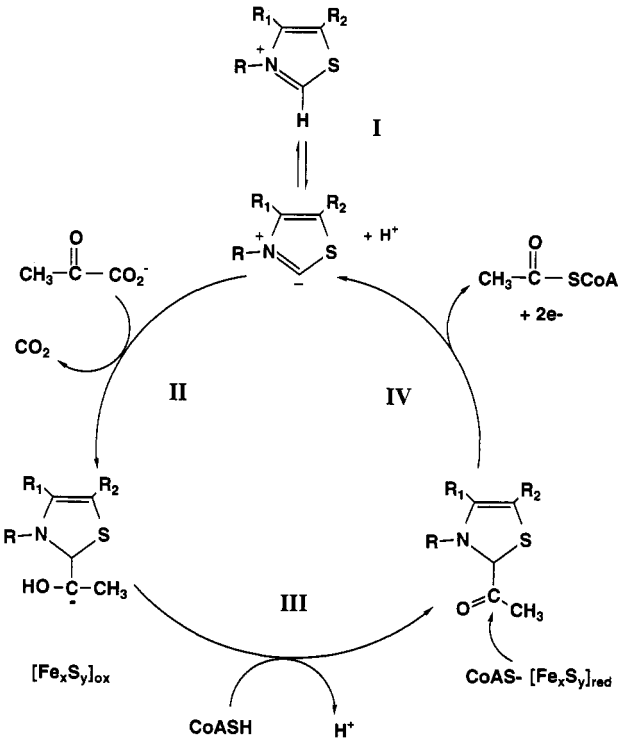

FeS center in Tm POR (Scheme 3). Copper in Pf POR is also proposed to play a role in substrate activation (Scheme 2). It should be noted that Schemes 2 and 3 represent tentative mechanisms, and although consistent with the spectroscopic data, several of their features remain unexplained. Nevertheless, they will be used as a framework for discussing the effects of the substrates, both individually and in combination, on the properties of the oxidized PORs.

Role of Pyruvate. The addition of pyruvate to oxidized Pf POR resulted in the formation of an organic radical intermediate (Figure 2). The EPR signal from this species was broadened by the presence of pyruvate-2-^{13}C (Figure 6), suggesting that it arises from an HETPP radical intermediate. Hence, Pf POR is apparently another example in the growing list of enzymes that contain radical intermediates derived from substrates, coenzymes, or amino acid residues [see, for example, Edmondson (1978), Stubbe (1989), Frey (1990), and Ballinger *et al.* (1992)].

The appearance of the putative TPP radical species upon pyruvate addition to oxidized Pf POR was accompanied by the oxidation of the copper site. Thus, an HETPP radical and a Cu^{2+} species are depicted in Scheme 2 as the products of pyruvate decarboxylation (step II). However, except for a low concentration of Cu^{2+} (0.2 spin/mol), the electrons in both pyruvate and oxidized Pf POR are initially paired, so that the formation of the HETPP radical (step II) must involve another unpaired electron. Since the appearance of the radical is linked to an increase in the oxidation of the copper center (approximately 0.7 spin/mol), as shown by the increase in signal intensity at $g = 2.073$ (compare Figures 1a and 2a), the electron that is unaccounted for is most likely associated with the copper site itself.

In order for the copper site in oxidized Pf POR to become more oxidized upon pyruvate addition, it seems reasonable to speculate that the copper site is associated with a preexisting

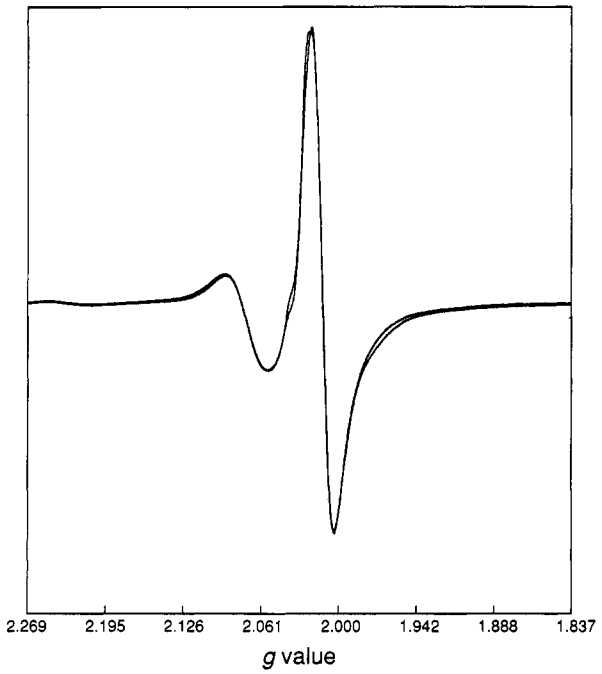

FIGURE 6: EPR spectra of oxidized Pf POR in the presence of 20 mM sodium pyruvate and 20 mM sodium pyruvate-*2*-^{13}C in 50 mM Tris-HCl (pH 8) and recorded at 12 K. The broadening of the spectrum arising from the addition of pyruvate-*2*-^{13}C is indicated by arrows. Experimental conditions were as follows: microwave power, 10 mW; modulation amplitude, 5 G; microwave frequency, 9.44 GHz; gain of 2.5×10^4.

stable radical within the protein. This would be analogous to the coupled copper/tyrosyl radical system ($Cu^+/R^\bullet$) found in galactose oxidase (Babcock *et al.*, 1992), except that in Pf POR it can be represented as follows:

$$Cu^{2+} + R^\bullet \Leftrightarrow Cu^+ + R$$

This type of association would then explain (a) the low spin quantitation for the Cu^{2+} site in the oxidized enzyme and (b) the increase in the Cu(II) signal that is observed upon the addition of pyruvate (Scheme 2, step II). Unfortunately, this hypothetical organic radical associated with oxidized Pf POR cannot be identified from the data presented herein. Of course, a likely candidate is TPP itself, and for the purpose of mechanistic comparisons, a $Cu^{2+}/TPP^\bullet$ site is shown for oxidized Pf POR in Scheme 2. In fact, a homolytic cleavage of the HETPP radical formed by pyruvate addition (Scheme 2, step II) would ultimately be required to form acetyl-CoA (step IV), and this would generate the Cu^{2+}/TPP-based radical in the absence of substrate. Moreover, after the formation of acetyl-CoA, the enzyme would be regenerated for further catalysis. The problem is that a TPP radical such as that proposed in the oxidized Pf enzyme would be unprecedented, especially a carbocation radical, and the exact mechanism by which it is generated is not clear. As yet we have been unable to remove the copper from the enzyme to determine whether the putative radical is still present, although the copper site might be the key to its formation and stabilization. On the other hand, the hypothetical stable radical in oxidized Pf POR might be associated with an amino acid side chain, as such species have been recently been identified in several proteins (Wagner *et al.*, 1992; Reichard & Ehrenberg, 1983; Bender *et al.*, 1989; Karthein *et al.*, 1988; Debus *et al.*, 1988; Whittaker & Whittaker, 1990; Babcock, 1992). Clearly, further investigations into the nature of the catalytic site in oxidized Pf POR are required, and these are underway.

Whatever the nature of the copper site and TPP in oxidized Pf POR, it is reasonable to conclude from the data that treatment with pyruvate generates an HETPP radical, as shown in Scheme 2. A substrate-induced TPP radical intermediate has also been reported in 2-oxo acid:ferredoxin oxidoreductase from the archaeon *H. halobium* (Kerscher & Oesterhelt, 1980). In addition, a radical species was detected in the untreated, oxidized *H. halobium* enzyme, and this was quenched by incubation with CoASH. This suggests the preexistence of an organic radical in this protein, just as we propose for Pf POR. After incubation of the *H. halobium* enzyme with pyruvate, the additional electron generated by the formation of the hydroxyalkyl-TPP radical was proposed to be transferred to an iron–sulfur center (Kerscher & Oesterhelt, 1980). However, this was not demonstrated experimentally and is not the case with Pf POR, as there was no evidence for a reduced FeS center in the pyruvate-treated enzyme. Whether the *H. halobium* enzyme also contains copper remains to be determined.

In Pf POR, an interesting speculation is that the copper atom replaces the divalent cation (Mg^{2+} or Mn^{2+}) typically associated with the diphosphate group of the TPP cofactor (R_2 group of TPP shown in Scheme 2; Muller & Schulz, 1993; Dyda *et al.*, 1993). The metal ion is bound in an octahedral arrangement to an oxygen atom of each phosphate group, as well as to a water molecule and other oxo ligands of amino acid side chains. The EPR spectrum of Pf POR shown in Figure 5 is characteristic of a copper atom coordinated by oxo ligands in an octahedral geometry, a type 2 copper center. Additional information concerning the coordination of the copper center is currently being investigated by X-ray absorption spectroscopy.

In contrast to Pf POR, a radical species was not observed in Tm POR when the oxidized enzyme was incubated with pyruvate, suggesting that its reaction mechanism follows conventional TPP chemistry, as depicted in Scheme 3 (step II). Interestingly, hydroxyalkyl-TPP radical intermediates have only been proposed in the keto acid oxidoreductases from *P. furiosus* (this study) and *H. halobium* (Kerscher & Oesterhelt, 1980), both of which are archaea, whereas an analogous radical species has not been found in the PORs from bacteria, which include *T. maritima* (this study), *Klebsiella pneumoniae* (Shah *et al.*, 1983), and *Clostridium thermoaceticum* (Wahl & Orme-Johnson, 1987). Although the presence or absence of copper was not reported in any of the mesophilic keto acid oxidoreductases, we would predict that this element is not present in the bacterial enzymes and that their catalytic mechanism is very similar to that of Tm POR, as described below.

Role of CoASH. In the pyruvate dehydrogenase complex, the nucleophilic attack on a lipoic acid-bound intermediate by CoASH results in the formation of acetyl-CoA (Scheme 1, step III). The question to be answered is how acetyl-CoA is formed from the HETPP radical in Pf POR (Scheme 2, step III) and from the HETPP intermediate in Tm POR (Scheme 3, step III). The EPR data showed that both Pf and Tm PORs undergo partial reduction upon incubation with CoASH. The following half-reaction represents the oxidation of CoASH, which is typically coupled to the reduction of a disulfide bond:

$$CoASH \Leftrightarrow CoAS + H^+ + e^-$$

With Pf POR, however, the oxidation of CoASH resulted in the complete reduction of the Cu^{2+} center (Figure 3a), as represented in Scheme 2 (step III). Hence, instead of a

nucleophilic attack by CoASH (see Scheme 1, step III), the formation of acetyl-CoA by Pf POR is proposed to occur after the prior oxidation of CoASH, as shown in Scheme 2 (step IV).

In Tm POR, on the other hand, the oxidation of CoASH was coupled to the reduction of a specific iron–sulfur center. Coincidentally, it was proposed, although not experimentally demonstrated, that in both *C. thermoaceticum* and *K. pneumoniae* PORs a thiol ligand from a [4Fe–4S] center might oxidize CoASH to generate a disulfide bond and that the same iron–sulfur center then becomes the final electron acceptor (Wahl & Orme-Johnson, 1987). Alternatively, CoASH could be oxidized by binding directly to an Fe atom of an FeS cluster, and likewise the cluster serves as the electron acceptor. We attempted to test these proposals but were unable to bind cyanide to Tm POR, which suggests the absence of a readily accessible (non-cysteinyl-ligated) Fe site. We were also unable to reduce *P. furiosus* ferredoxin, an atypical iron–sulfur protein, as its 4Fe center can coordinate an exogenous ligand, with CoASH. In any event, as shown in Scheme 3, it appears that the oxidation of CoASH in Tm POR is related to and leads to the reduction of a specific FeS center and that this center plays a catalytic role analogous to that of the Cu site in Pf POR (Scheme 2). Although it cannot be established from the data presented here exactly how acetyl-CoA formation is catalyzed by Tm POR (Scheme 3, steps III and IV), the spectroscopic results clearly support a reaction mechanism involving the interaction between CoASH and a unique FeS center. Hence, Pf POR appears to have a Cu/TPP radical-based mechanism for pyruvate oxidation, while Tm POR utilizes an FeS/TPP-based chemistry to catalyze the identical reaction.

Role of Pyruvate and CoASH. The two electrons generated from the oxidation of pyruvate (pyruvate/acetyl-CoA couple, $E^{\circ\prime} = -560$ mV) appear to each ultimately reduce one of the conventional $[4Fe–4S]^{2+}$ clusters present in the oxidized forms of both Pf and Tm PORs. Hence, the addition of both CoASH and pyruvate resulted in the apparent reduction of two iron–sulfur centers in each enzyme as determined by EPR analysis (Figure 4). For at least one of the iron–sulfur centers to be reduced in Pf POR, an electron generated from Scheme 2 (step III) must be transferred from the Cu^{+} center to a $[4Fe–S]^{2+}$ center. However, in order for electron transfer to take place, the copper center must have a midpoint potential comparable to that of a ferredoxin-type [4Fe–4S] cluster, which would be unprecedented. In addition, one would also expect the EPR signal of the oxidized Cu^{2+} center to be observed from the pyruvate/CoASH-treated enzyme, but this was not the case (even at 30 K, see Figure 4a). Since a large excess of both substrates was added to reduce the enzyme, it is possible that the copper site was subsequently reduced by CoASH after the formation of acetyl–CoA. Hence, in addition to the nature of the catalytic site of the oxidized Pf enzyme, it is not possible at present to clearly explain the fate of each electron generated from the oxidation of pyruvate, although ultimately they reduce two $[4Fe–4S]^{2+}$ clusters.

In contrast to Pf POR, we conclude that Tm POR contains two conventional ferredoxin-type [4Fe–4S] clusters and a third FeS center that specifically oxidizes CoASH. A comparison of the spectra of the dithionite-reduced (Figure 7), pyruvate/CoASH-reduced (Figure 4b), and CoASH-reduced (Figure 3b) forms of Tm POR shows that there is an unusual cluster in this enzyme that is specifically reduced when CoASH is the sole reductant. Its spectrum (the $g = 2.07$ signal) was not seen, however, in the pyruvate/CoASH-reduced enzyme. This

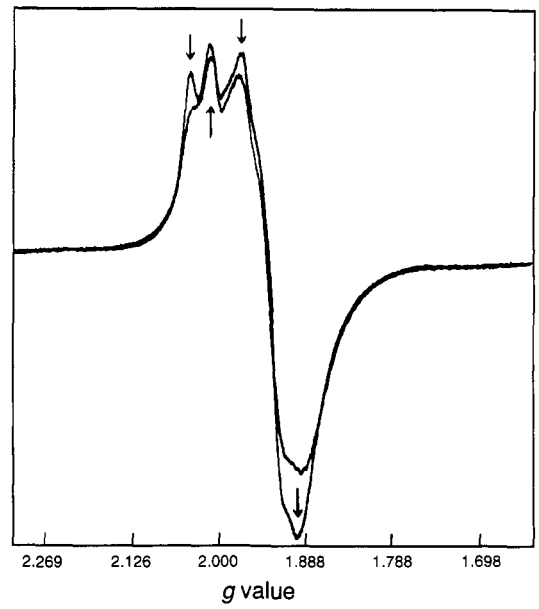

FIGURE 7: EPR spectra of Tm POR reduced with 20 mM dithionite in the presence and absence of 20 mM CoASH in 50 mM Tris-HCl (pH 8). The spectrum of Tm POR reduced by dithionite alone is indicated by arrows. Experimental conditions were as follows: 8 K; microwave power, 20 mW; modulation amplitude, 5 G; gain of 2.5×10^4.

suggests that CoASH binds to the enzyme and reduces its specific FeS cluster, which in turn reduces one of the conventional clusters, but that the CoASH-specific cluster cannot be rereduced (by excess CoASH) until the conventional 4Fe cluster(s) are oxidized (which requires an external electron carrier). However, as with Pf POR, the exact mechanism by which electrons are transferred in Tm POR from pyruvate to the [4Fe–4S] clusters is not clear. The presence of an additional FeS cluster in Tm POR compared to Pf POR is consistent with the measured Fe contents of these enzymes (approximately 10 and 8 Fe atoms/mol, respectively). These data also suggest that the CoASH-oxidizing cluster of Tm POR might be a 2Fe cluster (for a total of 10 Fe atoms/mol) rather than a 4Fe cluster (12 Fe atoms/mol). Additional spectroscopic analyses, e.g., magnetic circular dichroism or resonance Raman, are required to distinguish between these possibilities. In any event, with both Tm and Pf PORs, the data suggest that CoASH cannot simply be a nucleophile reacting with a bound intermediate, as proposed for the pyruvate dehydrogenase complex (Scheme 1, step III).

SUMMARY

A qualitative summary of the oxidation states of the redox centers found in Pf and Tm PORs as deduced from the observed EPR spectral changes in their paramagnetic centers is shown in Schemes 2 and 3, respectively. However, several questions about the mechanism of each enzyme remain unanswered. For example, with Pf POR, further experimentation is clearly required to elucidate the nature of the catalytic site in the oxidized enzyme and the thermodynamics of the proposed electron transfer between the copper site and a [4Fe–4S] cluster. Similarly, in Tm POR, the nature of the novel iron–sulfur center that oxidizes CoASH will require additional spectroscopic analyses. Nevertheless, it is now clear that there are two distinct mechanisms by which pyruvate is oxidized by various PORs, and these differ from the TPP/lipoic acid-based chemistry of the pyruvate dehydrogenase complex. The archaeal POR-type enzymes appear to utilize a TPP radical-

based mechanism, which in the case of Pf POR also involves copper, whereas in the copper-free bacterial enzymes, a unique catalytic role is proposed for a novel iron–sulfur center involving more conventional TPP chemistry.

ACKNOWLEDGMENT

We thank Professor R. S. Phillips (University of Georgia) and Professor G. T. Babcock (Michigan State University) for helpful discussions.

REFERENCES

Aasa, R., & Vänngård, T. (1975) *J. Magn. Reson. 19*, 308–315.
Adams, M. W. W. (1992) *Adv. Inorg. Chem.* 38, 341–396.
Adams, M. W. W. (1993) *Annu. Rev. Microbiol.* 47, 627–658.
Adams, M. W. W., & Kelly, R. M., Eds. (1992) *Biocatalysis at Extreme Temperatures: Enzyme Systems Near and Above 100 °C*, American Chemical Society, Washington, D.C.
Adams, M. W. W., Jin, S.-L. C., Chen, J.-S., & Mortenson, L. E. (1986) *Biochim. Biophys. Acta 869*, 37–47.
Aono, S., Bryant, F. O., & Adams, M. W. W. (1989) *J. Bacteriol. 171*, 3433–3439.
Babcock, G. T., El-Deeb, M. K., Sandusky, P. O., Whittaker, M. M., & Whittaker, J. W. (1992) *J. Am. Chem. Soc. 114*, 3727–3734.
Blamey, J. M., & Adams, M. W. W. (1993) *Biochim. Biophys. Acta 1161*, 19–27.
Blamey, J. M., & Adams, M. W. W. (1994) *Biochemistry 33*, preceding article in this issue.
Bryant, F. O., & Adams, M. W. W. (1989) *J. Biol. Chem. 264*, 5070–5079.
Cammack, R., Kerscher, L., & Oesterhelt, D. (1980) *FEBS Lett. 118*, 271–273.
Conover, R. C., Kowal, A. T., Fu, W., Park, J.-B., Aono, S., Adams, M. W. W., & Johnson, M. K. (1990) *J. Biol. Chem. 265*, 8533–8541.
Conover, R. C., Park, J.-B., Adams, M. W. W., & Johnson, M. K. (1991) *J. Am. Chem. Soc. 113*, 2799–2800.
Dyda, F., Furey, W., Swaminathan, S., Sax, M., Farrenkopf, B., & Jordan (1993) *Biochemistry 32*, 6165–6170.
Edmondson, D. E. (1978) *Biol. Magn. Reson. 1*, 205–237.
Fiala, G., & Stetter, K. O. (1986) *Arch. Microbiol. 145*, 56–61.
Frey, P. A. (1990) *Chem. Rev. 90*, 1343–1357.
Guest, J. R., Cole, S. T., & Jeyaseelan, K. (1981) *J. Gen. Microbiol. 127*, 65–79.
Huber, R., Langworthy, T. A., Konig, H., Thomm, M., Woese, C. R., Sleytr, U. B., & Stetter, K. O. (1986) *Arch. Microbiol. 144*, 324–333.
Ito, N., Phillips, S. E. V., Stevens, C., Ogel, Z. B., McPherson, M. J., Keen, J. N., Yadav, K. D. S., & Knowles, P. F. (1991) *Nature 350*, 87–90.
Kerscher, L., & Oesterhelt, D. (1981) *Eur. J. Biochem. 116*, 595–600.
McPhail, D. B., & Goodman, B. A. (1984) *Biochem. J. 221*, 559–560.
Mukund, S., & Adams, M. W. W. (1991) *J. Biol. Chem. 266*, 14208–14216.
Muller, Y. A., & Schultz, G. E. (1993) *Science 259*, 965–967.
Reinards, R., Kubicki, J., & Ohlenbusch, H.-D. (1981) *Eur. J. Biochem. 120*, 329–337.
Solomon, E. I., & Lowery, M. D. (1993) *Science 259*, 1575–1581.
Stetter, K. O., Fiala, G., Huber, G., Huber, R., & Segerer, G. (1990) *FEMS Microbiol. Rev. 75*, 117–124.
Stubbe, J. A. (1989) *Annu. Rev. Biochem. 58*, 257–285.
Thauer, R. K., Jungerman, K., & Decker, K. (1977) *Bacteriol. Rev. 41*, 100–180.
Wahl, W. C., & Orme-Johnson, W. H. (1987) *J. Biol. Chem. 262*, 10489–10496.
Woese, C. R., Kandler, O., & Wheelis, M. L. (1990) *Proc. Natl. Acad. Sci. U.S.A. 87*, 4576–4579.
Wrba, A., Jaenicke, R., Huber, R., & Stetter, K. O. (1990a) *Eur. J. Biochem. 188*, 195–201.
Wrba, A., Schweiger, A., Schultz, V., Jaenicke, R., & Zavodszky, P. (1990b) *Biochemistry 29*, 7584–7592.